Journal of the Optical Society of Korea
Vol. 12, No. 3, September 2008, pp. 200-204

DOI: 10.3807/JOSK.2008.12.3.200

Temperature Dependent Terahertz Generation at Periodically Poled Stoichiometric Lithium Tantalate Crystal Using Femtosecond Laser Pulses

N. E. Yu*, C. Kang, H. K. Yoo, C. Jung, Y. L. Lee, C.-S. Kee, D.-K. Ko, and J. Lee

Nonlinear Optics Laboratory, Advanced Photonics Research Institute, Gwangju Institute of Science and Technology, Gwangju 500-712, Korea

(Received July 14, 2008 : revised August 11, 2008 : accepted August 11, 2008)

Coherent tunable terahertz generation was demonstrated in periodically poled stoichiometric lithium tantalate crystal via difference frequency generation of femtosecond laser pulses. Simultaneous forward and backward terahertz radiations were obtained around 1.35 and 0.63 THz, respectively at low temperature. By cooling the crystal to reduce losses caused by phonon absorptions, the generated THz bandwidth was as narrow as 23GHz at the center frequency of 0.63 THz. The measurement result of temperature-dependent showed gradual intensity increase of the generated terahertz pulse and red shift of the center frequency as the temperature decrease from 291 to 143 K, but insignificant reduction of the spectral bandwidth. Furthermore, the stoichiometric crystal was very suitable for the suppression of THz loss at low temperature compared to the congruent $LiNbO_3$ crystal.

Keywords : difference frequency generation, terahertz generation, quasi-phase matching

OCIS codes : (190.4410) Nonlinear optics, parametric processes ; (190.2620) Frequency conversion ; (130.3730) Lithium niobate

I. INTRODUCTION

Coherent terahertz (THz) radiation source has many potential applications such as spectroscopy, imaging, medical diagnostics, gas sensing, and astronomy [1-4]. Based on an ultrafast femtosecond (fs) laser two main methods are using for the generation of the ultrafast electromagnetic radiation in the THz range. One is high -speed photoconductive switching using a dipole antenna and the other is optical rectification (OR) using a nonlinear crystal.

Recently, an alternative approach for the tunable narrow-band THz generation which had multi-cycles or arbitrary wave forms was demonstrated using a periodically poled nonlinear crystal [5-6]. For the generation of multi-cycles of THz waves the main idea was to use the group velocity mismatch between the optical and THz waves in the periodically poled structure. In the medium the optical and the generated THz pulses will be separated after a walk-off length and then the optical pulse will lead the THz pulse by the optical pulse duration. If the poled domain length is comparable to the walk-off length, each poled domain contributes to the THz radiation independently. Because of the periodic reversed sign of the nonlinearity at each domain, the generated THz waves also had reversed wave forms alternatively.

In this work, we achieved simultaneously forward and backward THz generation by difference frequency generation (DFG) of a broadband fs laser, which allows the generation of narrow-band and multi-cycles THz wave forms. Generally to make THz radiation by DFG process, two laser sources have to be used at very close frequency in nanosecond (ns) pulse or continuous wave [7-8]. However, an advantage of this work is that only one pump laser such as a mode-locked fs laser which has several different frequencies was used for THz generation. The difference of frequencies among optical waves within the spectral range directly corresponds to the generated THz frequencies, and the grating wavevector of the poled crystal could be satisfied by simul-

*Corresponding author: neyu@gist.ac.kr

taneous forward and counter-propagating backward THz radiations by the wavevector conservation. Up to now, simultaneous measurement of the forward and backward THz generations in periodically poled nonlinear crystals was hard because of the low intensity and the high absorption loss of the backward signal. Here, we clearly observed both forward and backward THz radiations in the periodically poled stoichiometric lithium tantalate (PPSLT) for the first time, owing to the low defect density of the stoichiometric crystal [9]. Additionally, we proved the origin of narrow band THz radiation in the periodically poled structure by not OR but DFG process [9-10].

II. DIFFERENCE FREQUENCY GENERATION AND EXPERIMENTAL SET-UP

A broadband mode-locked fs laser pulse, which consists of several different frequencies such as ω_1 and ω_2, can induce the difference of the frequencies such as, ω_{THz} ($= \omega_1 - \omega_2$), assuming $\omega_1 > \omega_2$ in a nonlinear crystal. The generated THz frequency by DFG process can be described as follows: [9-10]

$$\vec{K}_{\omega THz} = \Delta\vec{K}_{DFG} - \vec{K}_{\Lambda} \quad (1)$$

where $\Delta\vec{K}_{DFG} = \vec{K}_{\omega 1} - \vec{K}_{\omega 2}$, $\vec{K}_{\omega 1}$ and $\vec{K}_{\omega 2}$ are the wave vectors of each frequency, and $\vec{K}_{\Lambda}$ is the grating wavevector of the periodically poled crystal, respectively. When we select ω_1 as a center frequency of a fs pulse, the DFG frequency can be varied according to ω_2 frequencies within the bandwidth of the fs pulse. And the grating wavevector of the poled structure precisely determines the THz frequency among the various DFG frequencies as the result of the phase velocity matching condition. Fig. 1 shows the calculated result of the THz frequency as a function of the domain length using reported material dispersions [11-12] at the center wavelength of pump laser of λ=800 nm.

It was hard to explain by the OR which was described in some previous reports [5-6]. The frequency ω_2 which is involved in the backward interaction of the DFG is always a little higher than that of the forward interaction so the grating wavevector of the crystal contributes to the opposite direction of the pump pulse. As a result, the backward THz radiation always occurs at shorter frequency compared to the forward because of the wavevector conservation. Therefore, by the two simultaneously conserved wavevector conditions THz radiations could be generated in both forward and backward directions as shown in Fig. 1. In the calculation the contributed frequency ω_2 was 374.4 THz for the backward and 373.6 THz for the forward at the fixed frequency ω_1 of 375 THz with the periodic poled domain length of 30 μm at room temperature.

Fig. 2 shows the experimental setup for THz generation at low temperature and detection by time-domain measurement. As the fs pump laser, a Ti:sapphire oscillator system (Mira-900, Coherent) with a repetition rate of 76 MHz and a pulse duration of 190 fs was utilized at the center wavelength of 800 nm with the spectrum bandwidth of 7 nm. The collimated pump beam with input power of 0.5 W was divided into two beams and the transmitted main beam was focused into the sample. The reflected pump beam with power about 1 mW was used as a probe beam for the THz detection through time-delay. The PPSLT sample was mounted on the homemade cold finger of a cryogenic system for low temperature operation. The emitted THz radiation was collected and focused by two off-axis parabolic mirrors onto the detector. The detector was a low temperature grown GaAs photoconductive antenna with a typical dipole gap of 5 μm. The stoichiometric $LiTaO_3$ crystal used was

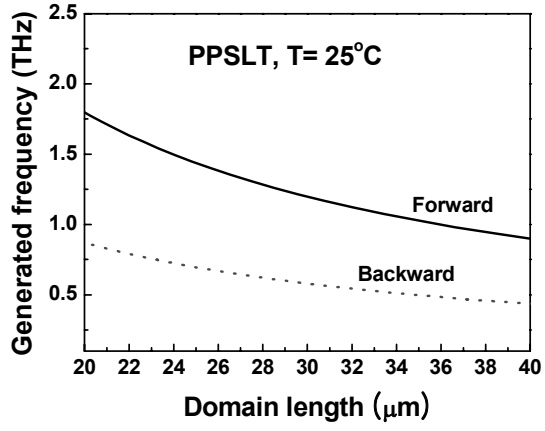

FIG. 1. Generated THz frequency via difference frequency generation as a function of the domain length in PPSLT at room temperature.

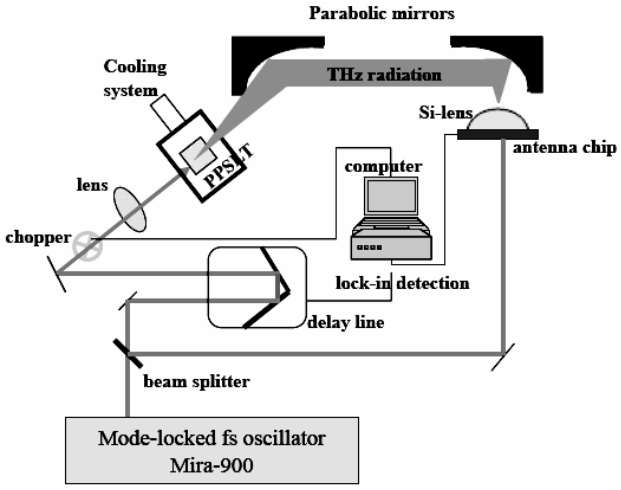

FIG. 2. Experimental setup for THz generation and detection at low temperature by time-domain measurement.

grown by the double-crucible Czochralski method [13]. Because of the significantly lower coercive field to make the periodically poled structure into the stoichiometric crystals, the 2 mm-thick PPSLT device was achieved by the electrical poling method [14].

III. EXPERIMENTAL RESULTS AND DISCUSSIONS

Schall and co-workers had reported the optical properties of $LiTaO_3$ and $LiNbO_3$ crystals from 0.1 to 3 THz [12]. They investigated the refractive index as 6.5 and the absorption coefficient as 70 cm^{-1} at 1.3 THz in congruent $LiTaO_3$, respectively. According to their report the main origin of the THz losses was the lowest transverse optical (TO) phonon resonance and higher order phonon process. The TO phonon could decay by coupling to weakly Raman-active relaxational modes and by scattering at crystal defects [15]. The TO coupling to low-frequency modes was weaker at low temperature. So cooling of the crystal was expected to suppress the THz absorption strongly.

The experiment was performed from room temperature to 130 K using liquid nitrogen and a vacuum chamber with cooling system. The measured THz signals in time -domain and corresponding spectra were shown in Fig. 3. As a first step we observed the THz waveforms with multi-cycles which were strongly attenuated through the propagation along the crystal length at T=291 K. However, at the next step the attenuated THz signal was recovered at lower temperatures from T=203 K to T=143 K. Furthermore the generated THz waves of each domain were clearly obtained and also two different frequencies were observed. At T=143 K, the generated THz waveform consists of 33 cycles with almost equal amplitudes. The 33 PPSLT domains (2-mm long with the periodically poled period of 60 μm) contributed to each cycle of generated THz waveform independently. Compared to the room temperature measurement, the spectrum bandwidth was narrowed while signal power was increased. Moreover, the counter-propagated backward signal was measured at lower frequency as well delayed in time without attenuation.

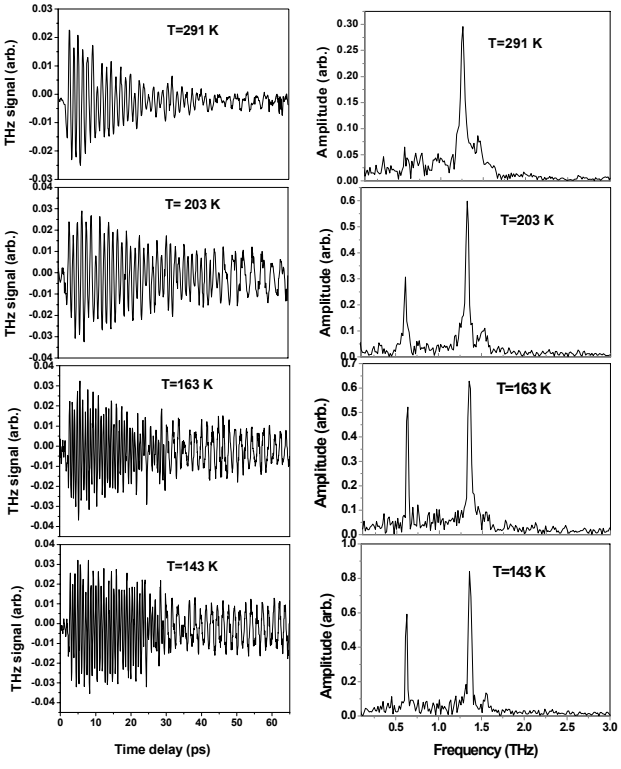

FIG. 3. Generated THz waveforms at time-domain and Fourier transformed spectra at each temperature.

Due to the large refractive index of the material at THz frequency range, we could measure the reflected backward THz signal at the front side. The counter-propagating THz signal should be delayed in time compared to the forward THz signal as much as the group velocity; 12 ps/mm of the crystal. The Fourier transformed spectra of Fig. 3 show both forward and backward THz generations of 1.35 and 0.65 THz, respectively, at the temperature T=143 K. The result is close to the expected frequency of THz radiation in the calculation result (see Fig 1). The THz spectrum bandwidth can be estimated as $\Delta\upsilon=2\ \upsilon/N$, where υ is the center frequency and N is the total number of domains. The spectrum bandwidth was as narrow as 33.7 GHz at T= 143 K and it became narrower at low temperature at the center frequency of 1.35 THz.

Here we used only one QPM period of 60 μm at PPSLT. If we change the QPM period from 30 to 80 μm the generated THz frequency can be tuned from 1.0 to 2.0 THz as shown in Fig. 1 at the forward direction. *Ito* and co-authors already reported the continuous THz -wave generation using a slanted-PPLN, and they demonstrated tunable THz-waves depending on QPM period [7]. Recently we also reported the tunable THz generation using a periodically poled fan-out structure in a $LiNbO_3$ crystal [16].

As shown in Fig. 3, the generated THz amplitudes, both forward and backward propagating, were dramatically increased as temperature decreased. Amplitude of THz signal of the forward propagating at T=143 K was about 3 times larger than that at T=291 K. It implies that the THz power could be about 9 times higher at the low temperature. For absolute power measurement of the generated THz-waves a Si-bolometer around 4 K is under preparation. The bandwidths of the spectra were 33.7, 33.8, and 40.0 GHz at T=143, 203, and 291 K, respectively. The small broadening of the THz spectrum was almost constant for the temperature below about 200 K, although the THz power increased substantially as the temperature decreased. It was also observed that the spectrum shifts to the red with decreasing

temperature. The center frequency was 1.35, 1.33, and 1.26 THz at T=143, 203, and 291 K, respectively. The frequency shift caused by the interplay of the temperature -dependent refractive index and the thermal expansion [17].

Note that THz absorption in congruent $LiNbO_3$ is about twice lower than that of the congruent $LiTaO_3$ around 0.5∼2.0 THz at room temperature. So to reduce the attenuation of THz-wave the crystal should be cooled down over the limit of liquid nitrogen temperature of 77 K, thus the cooling system had to use liquid helium to keep the crystal temperature below to 19 K [6]. However, here we achieved the effective suppression of the THz attenuation at relatively high temperature of about 143 K. It was very convenient, using liquid nitrogen with low cost, compare to the previous work [6]. A significant reason is that the used stoichiometric crystal has significantly low defect density compared to the congruent one, which results in lower scattering loss on the THz propagation. To directly prove this effect we are planning to do the similar work using congruent $LiTaO_3$ and will discuss later more detail.

IV. CONCLUSION

In summary, we have obtained simultaneous forward and backward THz radiations in PPSLT crystal. And analyzed the optical process of the THz generation by not OR but DFG. The generations of 1.35 and 0.63 THz with narrow bandwidths of 33.7 and 23 GHz, respectively, will make this a significant light source of coherent THz. At room temperature THz radiation was limited by THz absorption due to the TO phonon absorptions of the crystal. However, the THz absorption loss of the stoichiometric $LiTaO_3$ crystal was significantly suppressed at relatively high temperature of 143 K using low-cost liquid nitrogen compared to the congruent $LiNbO_3$ crystal which required high-cost liquid helium at extremely low temperature of 19 K. For potential application such as spectral density it is important that the narrow-band multi-wavelength THz source will be useful.

ACKNOWLEDGMENT

This work was supported by IITA of Korea through the 'Leading Edge R & D Program' and MEST of Korea through 'APRI-Research Program and Photonics 2020 of GIST'.

REFERENCES

[1] S. Nakajimam H. Hoshina, M. Yamashita, C. Otani, and N. Miyoshi, "Terahertz imaging diagnostics of cancer tissues with a chemometrics technique," *Appl. Phys. Lett.*, vol. 90, no. 4, pp. 041102-1∼041102-3, 2007.

[2] S. Hunsche, M. Koch, I. Brener, and M. C. Nuss, "THz near-field imaging," *Opt. Commun.*, vol. 150, no. 1998, pp. 22-26, 1998.

[3] C. Waschke, H. G. Roskos, R. Schwedler, K. Lep, H. Kurz, and K. Kohler, "Coherennt submillimeter-wave emission from Bloch oscillations in a semiconductor superlattice," *Phys. Rev. Lett.*, vol. 70, no. 21, pp. 3319-3322, 1993.

[4] M. Brucherseifer, M. Nagel, P. H. Bolivar, H. Kurz, A. Bosserhoff, and R. Buttner, "Label-free probing of the binding state of DNA by time-domain terahertz sensing," *Appl. Phys. Lett.*, vol. 77, no. 24, pp. 4049-4051, 2000.

[5] Y.-S. Lee, T. Meade, V. Perlin, H. Winful, T. B. Norris, and A. Galvanauskas, "Generation of narrow-band terahertz radiation via optical rectification of femtosecond pulses in periodically poled lithium niobate," *Appl. Phys. Lett.*, vol. 76, no. 18, pp. 2505-2507, 2000.

[6] Y.-S. Lee, T. Meade, M. DeCamp, T. B. Norris, and A. Galvanauskas, "Temperature dependence of narrow-band terahertz generation from periodically poled lithium niobate," *Appl. Phys. Lett.*, vol. 77, no. 9, pp. 1244-1246, 2000.

[7] Y. Sasaki, H. Yokoyama, and H. Ito, "Surface-emitted continuous-wave terahertz radiation using periodically poled lithium niobate," *Electro. Lett.*, vol. 41, no. 12, pp. 712-713, 2005.

[8] Y. J. Ding and W. Shi, "From backward THz difference -frequency generation to parametric oscillation," *IEEE J. Select. Topic. in Quant. Elec.*, vol. 12, no. 3, pp. 352-359, 2006.

[9] N. E. Yu, C. Jung, C.-S. Kee, Y. Lee, B.-A. Yu, D.-K. Ko, and J. Lee, "Backward terahertz generation in periodically poled lithium niobate crystal via difference frequency generation," *Jpn. J. Appl. Phys.*, vol. 46, no. 4A, pp. 1501-1504, 2007.

[10] N. E. Yu, C. Kang, H. K. Yoo, C. Jung, Y. Lee , C.-S. Kee, D.-K. Ko, J. Lee, K. Kitamura, and S. Takekawa "Simultaneous forward and backward terahertz generations in periodically poled stoichiometric $LiTaO_3$ crystal using femtosecond pulses," *Appl. Phys. Lett.*, vol. 93, no. 3, in press 2008.

[11] A. Bruner, D. Eger, M. B. Oron, P. Blau, M. Katz, and S. Ruschin, "Temperature-dependent Sellmeier equation for the refractive index of stoichiometric lithium tantalate," *Optics Lett.*, vol. 28, no. 3, pp. 194-196, 2003.

[12] M. Schall, H. Helm, and S. R. Keiding, "Far infrared properties of electro-optic crystals measured by THz time-domain spectroscopy," *Int. J. Infrared and Millimeter Waves* vol. 20, no. 4, pp. 595-604, 1999.

[13] Y. Furukawa, K. Kitamura, E. Suzuki, and K. Niwa "Stoichiometric $LiTaO_3$ single crystal growth by double crucible Czochralski method using automatic powder supply system," *J. Cryst. Grow.*, vol. 197, no. 98, pp. 889-895, 1999.

[14] N. E. Yu, S. Kurimura, Y. Nomura, M. Nakamura, K. Kitamura, Y. Takada, J. Sakuma, and T. Sumiyoshi, "Efficient optical parametric oscillation based on periodically poled 1.0mol% MgO-doped stoichiometric $LiTaO_3$," *Appl. Phys. Lett.*, vol. 85, no. 22, pp. 5134-5136, 2004.

[15] G. P.Wiederrecht, T. P. Dougherty, L. Dhar, K. A. Nelson, D. E. Leaird, and A. M. Weiner, " Explanation

of anomalous polariton dynamics in $LiTaO_3$," *Phys. Rev. B.*, vol. 51, no. 2, pp. 916 -931, 1995.

[16] C. Kang, C.-S. Kee, I.-B. Sohn, H. K. Yoo, Y. Lee, N. E. Yu, C. Jung, D.-K. Ko, and J. Lee, "Generation and transmission properties of THz pulses using periodic/ quasi-periodic structure," Proceeding of Advanced Lasers and Their applications workshop2008, Jeju, May1-3, pp. 50-51, 2008.

[17] N. E. Yu, C. Jung, C.-S. Kee, Y. Lee, B.-A. Yu, D.-K. Ko, J. Lee, W.-J. Lee, J.-E. Kim, and H. Y. Park "Terahertz generation in quasi-phase-matching structures using femtosecond laser pulses," *J. Korean Phys. Soc.* vol. 51, no. 2, pp. 493-497, 2007.